Establishment of a protoplast transformation method for the oleaginous yeast Rhodotorula toruloides

FEMS Yeast Research, 2026, **26**, foag028
https://doi.org/10.1093/femsyr/foag028
Published: 27 June 2026
Research article – Protocols, tools & methods

Establishment of a protoplast transformation method for the oleaginous yeast *Rhodotorula toruloides*

Xin Chen [1,2] **and Verena Siewers**[1,2,*]

[1]Division of Systems and Synthetic Biology, Department of Life Sciences, Chalmers University of Technology, SE-412 96 Gothenburg, Sweden
[2]Novo Nordisk Foundation Center for Biosustainability, Technical University of Denmark, DK-2800, Kgs. Lyngby, Denmark
*Corresponding author. Department of Life Sciences, Chalmers University of Technology, Kemivägen 10, SE-41296, Gothenburg, Sweden.
E-mail: siewers@chalmers.se
Editor: Hyun Ah Kang

Abstract

***Rhodotorula toruloides* is an oleaginous yeast with great potential for chemical and biofuel production, due to its ability to utilize lignocellulosic biomass and to produce high levels of carotenoids and storage lipids. However, its broader application in biotechnology has been limited by the lack of efficient genetic transformation methods. Although protoplast transformation is wildly used in fungal systems, it has remained largely unexplored in *R. toruloides*. In this study, we established a protoplast transformation protocol using linear DNA fragments and *R. toruloides* strain BOT-A2, a recently isolated strain with high lipid-producing potential. We first confirmed that BOT-A2 is a MAT A2 haploid strain. We then produced a β-1,3-glucomannanase (Man5C) that effectively digests the *R. toruloides* cell wall. Key parameters affecting transformation efficiency were systematically optimized, including the Man5C digestion conditions, antibiotic selection pressure, cell growth phase, protoplast yield and viability, PEG formulation, calcium ion concentration, and regeneration conditions. Using the optimized protocol, we successfully transformed BOT-A2 with three heterologous resistance cassettes (hygromycin R, bleomycin, and G418) yielding 190, 226, and 244 transformants per μg of DNA, respectively. This method provides a platform for genetic manipulation and is expected to facilitate both fundamental research and metabolic engineering in *R. toruloides* BOT-A2.**

Keywords protoplast transformation, *Rhodotorula toruloides*, BOT-A2, linear DNA fragment, oleaginous yeast

Introduction

The oleaginous yeast *Rhodotorula toruloides* is capable of naturally accumulating lipids exceeding 65% of its dry cell weight and has emerged as a promising microbial chassis for the production of diverse bioproducts, including carotenoids, terpenoids, and fatty-acid-derived compounds (Zheng et al. 2025). In addition to its high lipid content, *R. toruloides* can efficiently utilize both C5 and C6 sugars commonly derived from lignocellulosic biomass and exhibits strong tolerance to inhibitory compounds present in unrefined substrates. Its ability to grow well at low pH also helps reduce the risk of bacterial contamination (Hu et al. 2009, Geiselman et al. 2020). These features make *R. toruloides* particularly attractive for industrial scale bioproduction. In recent years, it has been engineered to synthesize various value-added compounds from lignocellulosic feedstocks, such as terpenoids, triacetic acid lactone, and fatty alcohols (Kirby et al. 2021, Cao et al. 2022, Schultz et al. 2022).

Despite its potential, metabolic engineering of *R. toruloides* remains significantly constrained by the lack of efficient and reliable genetic tools. Development of such tools is crucial to establish *R. toruloides* as a versatile microbial workhorse for industrial biotechnology. To date, four transformation methods have been reported for introducing exogenous DNA into *R. toruloides*: protoplast-mediated transformation (PMT) (Tully and Gilbert 1985), *Agrobacterium tumefaciens*-mediated transformation (ATMT) (Koh et al. 2014), electroporation (Liu et al. 2017), and the lithium acetate method (Tsai et al. 2017).

PMT was first reported in *R. toruloides* in 1985, when Tully *et al.* introduced the phenylalanine ammonia lyase (*PAL*) gene into strain MS7013 (Tully and Gilbert 1985). However, the method was found to be inefficient and the transformants showed poor genetic stability, likely due to the absence of a stable plasmid system. Consequently, no further studies have reported on its use in this species. PMT has been widely applied in fungi such as *Saccharomyces cerevisiae*, *Schizosaccharomyces pombe*, *Komagataella phaffii* (*Pichia pastoris*), *Kluyveromyces. lactis*, and *Candida albicans* (Hinnen et al. 1978, Sreekrishna et al. 1984, Cregg et al. 1985, Kurtz et al. 1986, Moreno et al. 1991). The standard transformation workflow involves enzymatic removal of the fungal cell wall to generate protoplasts, followed by treatment with calcium ions and polyethylene glycol (PEG) to facilitate DNA uptake (Gietz and Woods 2001). The protocol consists of multiple steps, each requiring strain-specific optimization (Fig. 1). Notably, the generation of

Received: 26 March 2026. **Revised:** 30 May 2026. **Accepted:** 22 June 2026

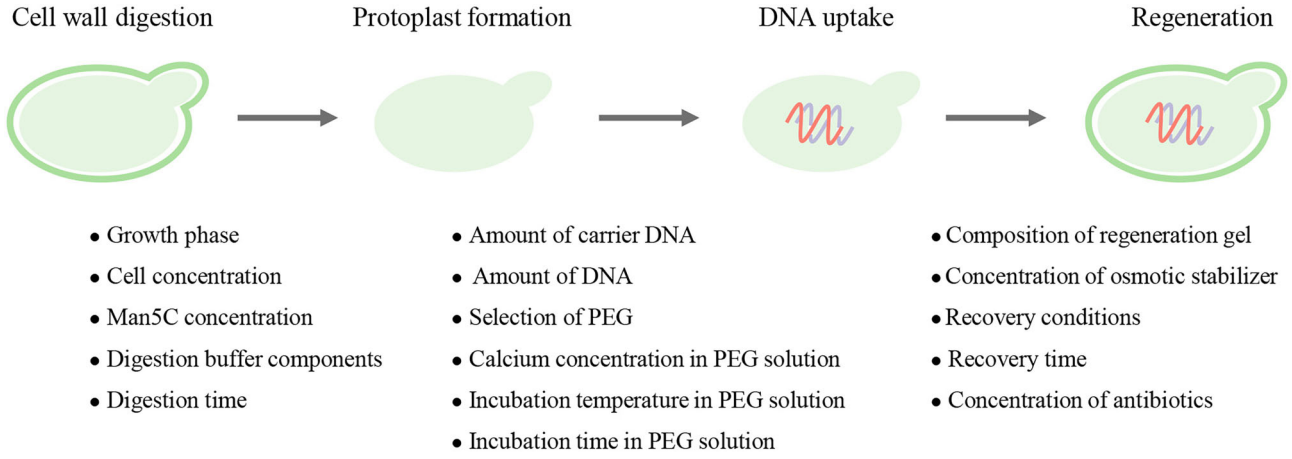

Figure 1 Key parameters to consider and optimize during the protoplast transformation process in *R. toruloides*.

high-quality protoplasts is often difficult to standardize due to the high variability in the fungal cell wall composition (Li et al. 2017). In *R. toruloides*, the lack of a functional episomal plasmid system further complicates the development of an efficient PMT workflow.

The *R. toruloides* strain BOT-A2 was recently isolated from leaves of exotic plants at the Gothenburg Botanical Garden in Sweden. This strain shows great potential as a lipid production host, exhibiting higher levels of storage lipid accumulation than commonly used strains and robust growth on a variety of substrates including glucose, xylose (a major component of lignocellulosic biomass), glycerol (a by-product of biodiesel production), and natural plant hydrolysate (Qvirist et al. 2022). More recently, Brink et al. (2023) generated a highly contiguous, functionally annotated genome for the BOT-A2 strain, collected RNAseq data and characterized six novel promoters (Brink et al. 2023). To harness the biotechnological potential of BOT-A2, an efficient genetic manipulation method is needed. In this study, we report the development of an efficient protoplast transformation protocol for introducing linear DNA fragments into *R. toruloides* BOT-A2.

Materials and methods

Strains and plasmids

All yeast strains and plasmids used in this study are specified in Supplementary Table 1. The natural yeast isolate *R. toruloides* BOT-A2 strain was kindly provided by Prof. Thomas Andlid (Chalmers University of Technology) and previously characterized (Qvirist et al. 2022). The *R. toruloides* Y4 and NP11 strains were kindly provided by Prof. Zongbao Kent Zhao (Dalian University of Technology) and previously described (Li et al. 2007, Zhu et al. 2012). The *Escherichia coli* DH5α strain was used for plasmid amplification. Three antibiotic resistance cassettes were amplified as follows: the pGPD-HYG-Tnos cassette was amplified from plasmid NM1-5S-tRNA-SgH using primers HYG-F/HYG-R, the pGPD-G418-Tnc cassette was amplified from plasmid NM9-SpCas9-NLS3 using primers G418-F/G418-R, and the pPGK-Ble-Tnos cassette was amplified from plasmid pZPK-SaCas9 using primers Ble-F/Ble-R. Primer sequences are listed in Supplementary Table 2. The NM1-5S-tRNA-SgH and NM9-SpCas9-NLS3 plasmids were gifts from Prof. Huimin Zhao (University of Illinois at Urbana-Champaign) (Addgene plasmid #128178; http://n2t.net/addgene:128178; RRID:Addgene_128178; Addgene plasmid #128177; http://n2t.net/addgene:128177; RRID:Addgene_128177) (Schultz et al. 2019). The pZPK-SaCas9 plasmid was kindly provided by Prof. Zongbao Kent Zhao (Jiao et al. 2019).

The *Pichia pastoris* strain X-33 and the expression plasmid pPICZα A were purchased from Invitrogen (Thermo Fisher Scientific). The codon-optimized *MAN5C* gene sequence was obtained from Yang et al. (Yang et al. 2011) and synthesized by Twist Bioscience (USA) for heterologous expression in *P. pastoris* X-33. The gene was cloned into the pPICZα A plasmid using Gibson assembly (New England Biolabs). The *MAN5C* fragment was amplified with primers MAN5C-F/MAN5C-R, and the pPICZα A backbone was amplified with primers PICZαA-F/pPICZαA-R. Primer sequences are listed in Supplementary Table 2. The resulting recombinant pPICZα A-MAN5C plasmid contained the *S. cerevisiae* α-factor secretion signal sequence, the *MAN5C* gene, and a C-terminal 6 $\times$ His tag sequence.

Culture conditions

Escherichia coli was cultivated in LB medium [10 g l^{-1} peptone from casein (Difco), 10 g l^{-1} NaCl, 5 g l^{-1} yeast extract] supplemented with either 100 μg ml^{-1} ampicillin (Sigma) or 50 μg ml^{-1} kanamycin (Sigma) at 37°C. *Rhodotorula toruloides* strains and *Pichia pastoris* X-33 were cultivated at 30°C with 220 rpm shaking unless specified explicitly. YPD medium contained 10 g l^{-1} yeast extract, 20 g l^{-1} peptone, and 20 g l^{-1} glucose. YNB medium contained 1.7 g l^{-1} YNB without ammonium sulphate (Formedium), 2.3 g l^{-1} K_2HPO_4, 11.83 g l^{-1} KH_2PO_4, 10 g l^{-1} ammonium sulphate, and 20 g l^{-1} glucose, adjusted to pH 5.5. For selection of transformants after protoplast transformation, YPD plates were supplemented with either 60 μg ml^{-1} hygromycin B (Thermo Fisher Scientific), 80 μg ml^{-1} G418 (Formedium), or 220 μg ml^{-1} zeocin (InvivoGen).

Yeast mating type assay

To determine the mating type of *R. toruloides* strains, a PCR-based assay targeting the mating pheromone receptor genes *STE3.A1* and *STE3.A2* was performed as described previously (Lopes et al. 2023). The Blood & Cell Culture DNA Kit (QIAGEN) was used to extract high molecular weight genomic DNA from 12 OD_{600} of

mid-exponential phase cells (OD_{600} of 3–3.5). PCR reactions were carried out using 20 ng of genomic DNA as template. The *STE3.A1* and *STE3.A2* gene fragments were amplified using the primer pairs STE3.A1-F/STE3.A1-R and STE3.A2-F/STE3.A2-R, respectively. Primer sequences are provided in Supplementary Table 2.

Cell size assay

Cells were cultured overnight at 30°C in 2 ml YPD medium and analyzed using a Guava easyCyte™ flow cytometer (Luminex). Forward scatter (FSC) signals were recorded using logarithmic amplifiers (FSC-Hlog), and 5000 events were analyzed per sample. FSC-Hlog was used as a relative indicator of cell size. In parallel, cells were imaged using an inverted microscope (Leica DMI4000 B). Cell diameters were quantified using ImageJ (NIH), with at least 400 cells measured per sample. Correlation analysis between microscopy-based cell diameters and FSC-Hlog values confirmed that FSC-Hlog increased with cell diameter under the applied instrument settings, validating its use as a proxy for relative cell size distribution.

Determination of yeast ploidy

Rhodotorula toruloides strains were cultivated in 2 ml YPD medium overnight at 30°C. A total of 0.5 OD_{600} of mid-exponential phase cells (OD_{600} of 3–3.5) were harvested and fixed in 1 ml of 70% ethanol at room temperature for 1 h. Fixed cells were stained with propidium iodide (Invitrogen) and analyzed using a FACS SH800 (Sony) as previously described (Todd et al. 2018) with slight modifications. Fixed cells were washed twice with 50 mM sodium citrate buffer and ultra-sonicated for 4 × 10 s at 10% of amplitude (Branson Ultrasonics) to separate cells. After centrifugation at 500 g for 10 min, cells were resuspended in 200 μl of 50 mM sodium citrate buffer containing 0.5 mg ml^{-1} RNase A (Thermo Fisher Scientific) and incubated at 37°C for 2 h. A 15 μl aliquot of unstained cells from each strain was reserved as a negative control for FACS measurement. To the remaining 185 μl of cell suspension, 5 μl of 1 mg ml^{-1} propidium iodide (Thermo Fisher Scientific) and 10 μl of 50 mM sodium citrate buffer were added, resulting in a final propidium iodide concentration of 25 μg ml^{-1}. Samples were incubated overnight at 37°C in the dark and sonicated for 10 s at 10% of amplitude prior to analysis. FACS analysis was performed using a 615/25 filter at an event rate of ∼1000 cells per second. A minimum of 20 000 events were taken per sample to ensure statistical robustness. The diploid *R. toruloides* Y4 strain and the haploid NP11 strain were used as controls to determine the ploidy of BOT-A2. Autofluorescence was verified to be minimal by analyzing unstained yeast cells.

Expression and purification of Man5C

The pPICZα A-MAN5C plasmid was linearized using the restriction enzyme *Sac*I (Thermo Fisher Scientific) and used to transform *P. pastoris* X-33 by electroporation at 1.5 kv, 25 μF, 200 Ω in a 0.2-cm electroporation cuvette using a Gene Pulser system (BioRad). Following transformation, cells were plated on YPD plates containing 1 M sorbitol and 100 μg ml^{-1} zeocin (InvivoGen) for selection. Gene integration was verified by colony PCR using the AOX1-F/AOX1-R primers (Supplementary Table 2). To assess Man5C protein expression, positive colonies were cultured in 2 ml of BMGY medium (10 g l^{-1} yeast extract, 20 g l^{-1} peptone, 3 g l^{-1} K_2HPO_4, 11.8 g l^{-1} KH_2PO_4, 1.34% YNB, 4 × 10^{-5}% biotin, and 1% glycerol) at 30°C overnight. 20 OD_{600} of cells were harvested at 3000 g for 5 min and then resuspended in 20 ml of BMMY medium (10 g l^{-1} yeast extract, 20 g l^{-1} peptone, 3 g l^{-1} K_2HPO_4, 11.8 g l^{-1} KH_2PO_4, 1.34% YNB, 4 × 10^{-4} g l^{-1} biotin, and 0.5% methanol) to an initial OD_{600} of 1. Cultures were incubated at 30°C for 96 h with 0.5% methanol added every 24 h to induce protein expression.

Cultures were centrifuged at 4,700 rpm for 10 min at 4°C, and the supernatant was collected and concentrated 35-fold using protein concentrators with a 10 kDa MW cutoff (PES, Thermo Fisher Scientific). The 6 × His tagged Man5C protein was purified from the concentrated supernatant using Ni-NTA agarose beads (Qiagen), prepared as a 50% slurry of TALON 6 × His affinity resin. A total of 0.5 ml of resin was loaded into a gravity column and equilibrated with 5 × 1 ml of TNG buffer (50 mM Tris-HCl, pH 7.5, 100 mM NaCl, 10% glycerol). Two milliliters of the concentrated supernatant were incubated with the equilibrated resin on a roller at 4°C for 1 h. The resin was washed twice with 1 ml of TNG buffer supplemented with 30 mM imidazole, and the bound protein was eluted with 1 ml of TNG buffer supplemented with 300 mM imidazole. Eluted protein was desalted using PD-10 columns (GE Healthcare) and stored at −80°C in 45% glycerol as aliquots.

Protein concentration was determined using a NanoDrop spectrophotometer (Thermo Fisher Scientific), and purity was evaluated by SDS-PAGE. Aliquots of the concentrated supernatant and purified protein were loaded onto a 4%–20% Mini-PROTEAN TGX Stain-Free Protein Gels (Bio-Rad) and visualized using the Gel Doc EZ imaging system (BioRad).

Protoplast transformation

Cell cultivation

Three fresh colonies of *R. toruloides* BOT-A2 were used to inoculate 2 ml of YPD medium and grown overnight at 30°C. The overnight culture was then diluted to an initial OD_{600} of 0.002 in 20 ml of YPD medium in a 100 ml shake flask. Cells were grown at 30°C for 12-18 h and harvested at one of the following growth phases: early exponential phase (OD_{600} of 1–1.5), mid-exponential phase (OD_{600} of 3–3.5), or late-log phase (OD_{600} of 6–6.5).

Protoplast preparation

15 OD_{600} of cells were transferred to a 50-ml falcon tube and centrifuged at 3000 g for 5 min at 4°C, yielding sufficient cells for 2 transformation reactions. The cell pellet was washed once with 10 ml of sterile Milli-Q water and resuspended in 2 ml of digestion buffer containing 10 mM sodium acetate buffer (pH 4.5), 1 M sorbitol (Sigma), and purified Man5C protein (1.12 μg ml^{-1}). The OD_{600} was measured after diluting the cell suspension 20-fold in 1 M sorbitol. Digestion was carried out at 37°C in a ThermoMixer (Eppendorf) with shaking at 300 rpm. After 15 min, 50 μl of the digested cells were mixed with 950 μl of 1% SDS to assess protoplast formation. Digestion was terminated when the OD_{600} ratio, comparing values before Man5C digestion (cells diluted in 1 M sorbitol) and after digestion (cells diluted in 1% SDS), reached ∼10 or 20. Protoplasts were immediately transferred to 10 ml of ice-cold 1 M sorbitol using a wide-bore 1 ml pipette tip which was prepared by cutting the end of a standard tip to minimize the shear damage to protoplasts. After centrifugation at 700 g for 8 min at 4°C, the

supernatant was carefully decanted, and the protoplasts were gently rinsed with 10 ml of ice-cold 1 M sorbitol. Finally, protoplasts were resuspended in 200 μl of STC buffer (1 M sorbitol, 10 mM Tris HCl, pH 7.5, 10–50 mM $CaCl_2$) using a wide-bore 200 μl pipette tip. The specific $CaCl_2$ concentrations used in the STC buffer are shown in Fig. 4.

Transformation procedure

For each transformation, 100 μl of protoplast suspension was mixed with no more than 5 μl of linear DNA fragments (~1 μg per kb) and 5 μl of carrier DNA (Takara) using a wide-bore 200 μl pipette tip. The mixture was incubated at room temperature (20°C) for 15 min. Then, 1 ml of PEG buffer containing either 40% (w/v) PEG 4000 (Sigma) or 20% (w/v) PEG 8000 (Sigma), 10 mM Tris HCl, pH 7.5, 10–50 mM $CaCl_2$ was added, and the tube was gently inverted 8–10 times to mix. The sample was incubated at room temperature (20°C) for 20 min, then centrifuged at 700 g for 8 min at 4°C. The supernatant was carefully removed, and the protoplasts were gently resuspended in 1.5 ml of SOS buffer (6.5 mM $CaCl_2$, 0.25% yeast extract, 0.5% peptone, 1 M sorbitol) using a wide-bore 1 ml pipette tip in a 14-ml culture tube. The tubes were incubated at 30°C without shaking for 1 h, followed by shaking at 200 rpm for 2 h. Afterwards, 1 ml of YPD medium supplemented with 1 M sorbitol was added, and incubation with shaking continued for 2 h. Subsequently, 2.5 ml of YPD medium supplemented with 1 M sorbitol was added, and the suspension was divided into two tubes. Cells were incubated for an additional 14–16 h at 30°C with shaking at 200 rpm. Following recovery, 500 μl of each culture was plated on YPD plate containing the appropriate antibiotic. Plates were incubated at 30°C for 4–8 days. The effects of transformation temperature and $CaCl_2$ concentration in PEG buffer were examined as described in Fig. 4.

Genetic stability analysis of transformants

After protoplast transformation, individual transformants were grown in 1 ml YPD medium supplemented with the appropriate antibiotics overnight at 30°C to recover transformants and eliminate any potential false positives. After overnight growth, 10 μl of the culture was transferred into 2 ml of fresh YPD medium and incubated at 30°C for 24 h. This process was repeated for five consecutive generations. After the fifth generation, the cultures were plated on YPD plates containing antibiotics to assess whether the transformants retained antibiotic resistance and maintained genetic stability.

PCR verification of genetic integration

After overnight cultivation, 0.5 OD_{600} of cells were taken and washed once with 1 ml deionized H_2O. The pellet was resuspended in 100 μl digestion buffer containing 10 mM sodium acetate buffer (pH 4.5), 1 M sorbitol, and purified Man5C protein (1.12 μg ml^{-1}). The suspension was incubated at 37°C for 30 min in a ThermoMixer (Eppendorf) with shaking at 300 rpm. Following digestion, cells were collected by centrifugation at 700 g for 10 min at 4°C, resuspended in 30 μl of deionized H_2O, and then boiled for 20 min to release genomic DNA. After centrifugation, 0.5 μl of the supernatant was used as the template for PCR using primers HYG-seq-F/R (Supplementary Table 2).

Growth analysis

Growth analysis was performed in YPD and YNB medium. For both *R. toruloides* BOT-A2 and NP11 strains, three individual colonies were used to inoculate 2 ml of YPD or YNB medium and cultured overnight at 30°C. The overnight cultures were then diluted into 1 ml of fresh YPD or YNB medium to an initial OD_{600} of 0.1. Cell growth was monitored using a BioLector microcultivation system (m2p-labs).

Statistical methods

Data were presented as mean ± standard deviation (SD). Statistical significance was assessed using a two-tailed Student's *t*-test assuming equal variance, as identical procedures were used to determine all parameters. Unless otherwise stated, data analysis was based on three biological replicates. A P value < 0.05 was considered statistically significant unless specified otherwise.

Results

Mating type and ploidy of BOT-A2 strain

The *R. toruloides* BOT-A2 strain has a genome size of 20.54 Mb, assembled into 20 contigs (Brink et al. 2023). Previous studies have reported that substantial genomic differences between haploid *R. toruloides* strains of different mating types (MAT A1 vs. MAT A2) (Hu and Ji 2016, Sambles et al. 2017). Based on average nucleotide identity (ANI) and pheromone receptor analysis, BOT-A2 clusters within the MAT A2 group, although its name was not chosen to reflect its mating type (Brink et al. 2023). In this study, the mating type was determined by PCR amplification of the pheromone receptor genes *STE3.A1* and *STE3.A2* from genomic DNA. In the diploid strain Y4, both *STE3.A1* and *STE3.A2* fragments were amplified. In contrast, only the *STE3.A1* fragment was detected in the haploid NP11 strain, which has been previously identified as MAT A1 (Zhu et al. 2012). For the BOT-A2 strain, only the *STE3.A2* fragment was amplified, confirming its classification as MAT A2 (Fig. 2A).

Previous work has shown that diploid cells are substantially larger than haploids cells, as observed by microscopy (Zhang et al. 2022). To compare cell sizes in our study, we analyzed exponentially growing cultures using flow cytometry. Forward-scatter measurement with logarithmic amplifiers (FSC-Hlog) revealed two distinct peaks: one corresponding to the larger Y4 cells, and another shared by BOT-A2 and NP11, indicating that BOT-A2 and NP11 had similar, smaller cell sizes (Fig. 2B). The average cell diameter of BOT-A2 was 4.64 ± 0.65 μm, closely matching that of NP11 (4.99 ± 0.66 μm), and significantly smaller than Y4 (9.79 ± 1.17 μm, P value < 0.001) (Fig. 2C).

Ploidy, defined as the number of sets of homologous chromosomes in a cell, was characterized by measuring single-cell DNA content using the fluorescent dye propidium iodide. The haploid NP11 strain exhibited two peaks on the histogram corresponding to the G1 phase (one copy, 1C) and G2 phase (two copies, 2C) of the cell cycle. The G2 peak of NP11 aligned with the G1 peak of the diploid Y4 strain, as both represent cells containing two copies of the genome. Accordingly, the G2 peak of the diploid Y4 strain corresponded to cells with four genome copies (4C). These results are consistent with previous reports that haploid NP11 was isolated

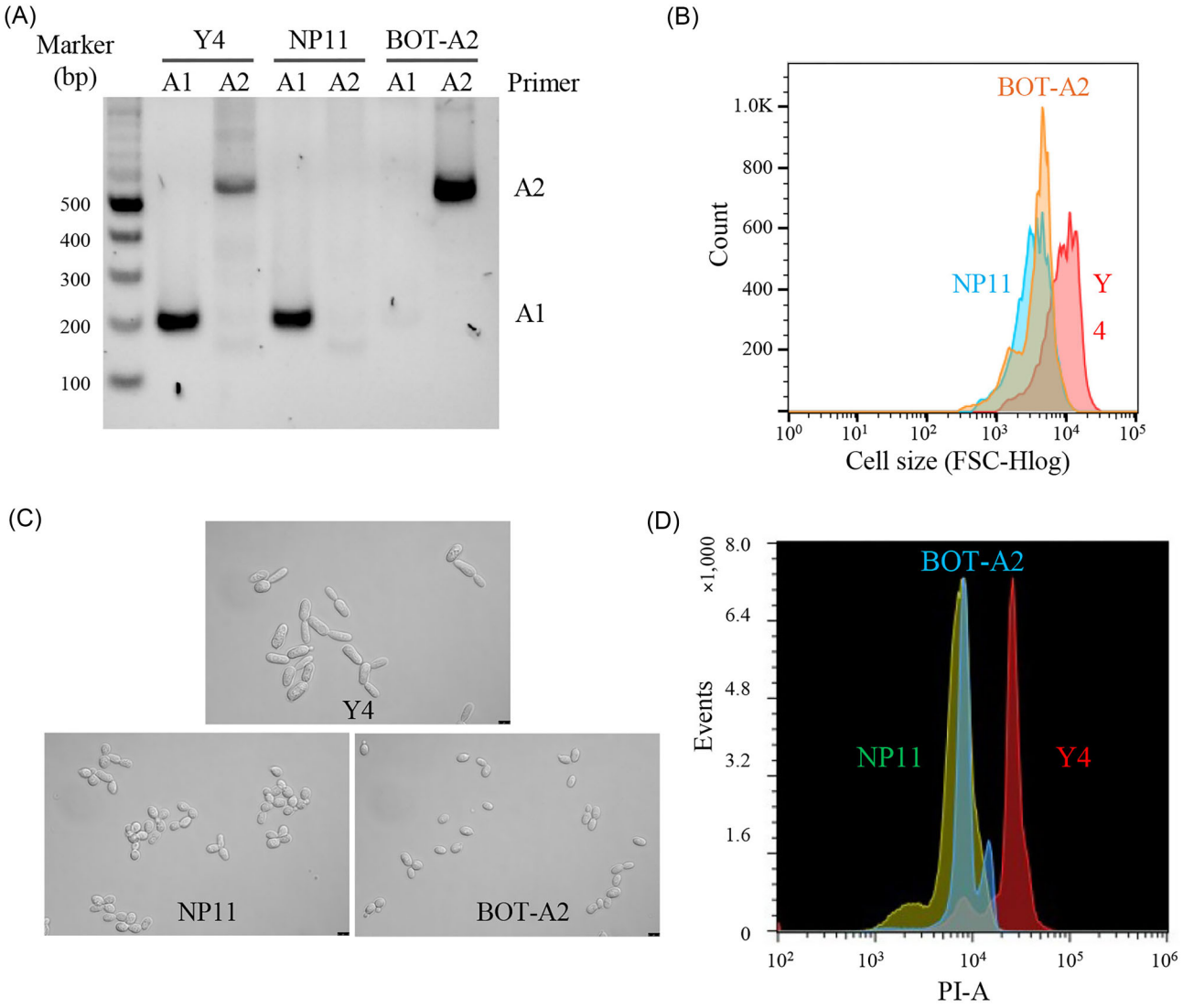

Figure 2 Determination of mating type and ploidy of *R. toruloides* BOT-A2. (A) PCR-based mating type analysis of the diploid strain Y4, haploid strain NP11, and BOT-A2. (B) Flow cytometry analysis of relative cell size distribution in Y4, NP11, and BOT-A2 strains based on forward scatter intensity (FSC-Hlog). (C) Phase-contrast micrographs of Y4, NP11, and BOT-A2 strains. Scale = 5 μm. (D) DNA content histograms based on propidium iodide staining (measured as fluorescence area) for Y4, NP11, and BOT-A2 strains.

from basidiospores germinated from teliospores of the diploid Y4 strain (Zhu et al. 2012).

The BOT-A2 strain also exhibited two major peaks corresponding to 1C and 2C DNA content (Fig. 2D and Supplementary Fig. 1), which were consistent with a haploid profile. Although the peak positions did not perfectly overlap with those of NP11, the assembled genome size of BOT-A2 (20.54 Mb) is comparable to that of the confirmed haploid NP11 strain (20.2 Mb). The shift in fluorescence peaks toward higher PI-A values relative to the haploid NP11 strain may be due to their distinct genetic backgrounds. Differences in fluorescence intensity and peak position might arise from strain-specific differences in chromatin accessibility, staining efficiency, growth conditions, and cell-cycle distribution. In addition, BOT-A2 did not display the characteristic 2C and 4C DNA content profile observed for the diploid Y4 strain, and its cell size was significantly smaller than that of the diploid Y4 strain (Fig. 2B and C). Together with the MAT A2-specific PCR result (Fig. 2A), these findings support classification of BOT-A2 as a MAT A2 haploid strain.

Expression of recombinant Man5C protein for protoplast generation

The cell wall of *R. toruloides* is primarily composed of glucomannan, which differs significantly from the glucan- and mannan–rich cell wall of *S. cerevisiae* (Antunes et al. 2024). As a result, *R. toruloides* is resistant to many commercially available lytic enzymes. Previous studies reported that the Man5C protein from *Penicillium lilacinus* ATCC 36010, which represents a β-1,3-glucomannanase, can effectively lyse the *R. toruloides* cell wall (Arai et al. 1978, Sugino et al. 2004). However, this enzyme is not commercially available. To address this limitation, we heterologously expressed a

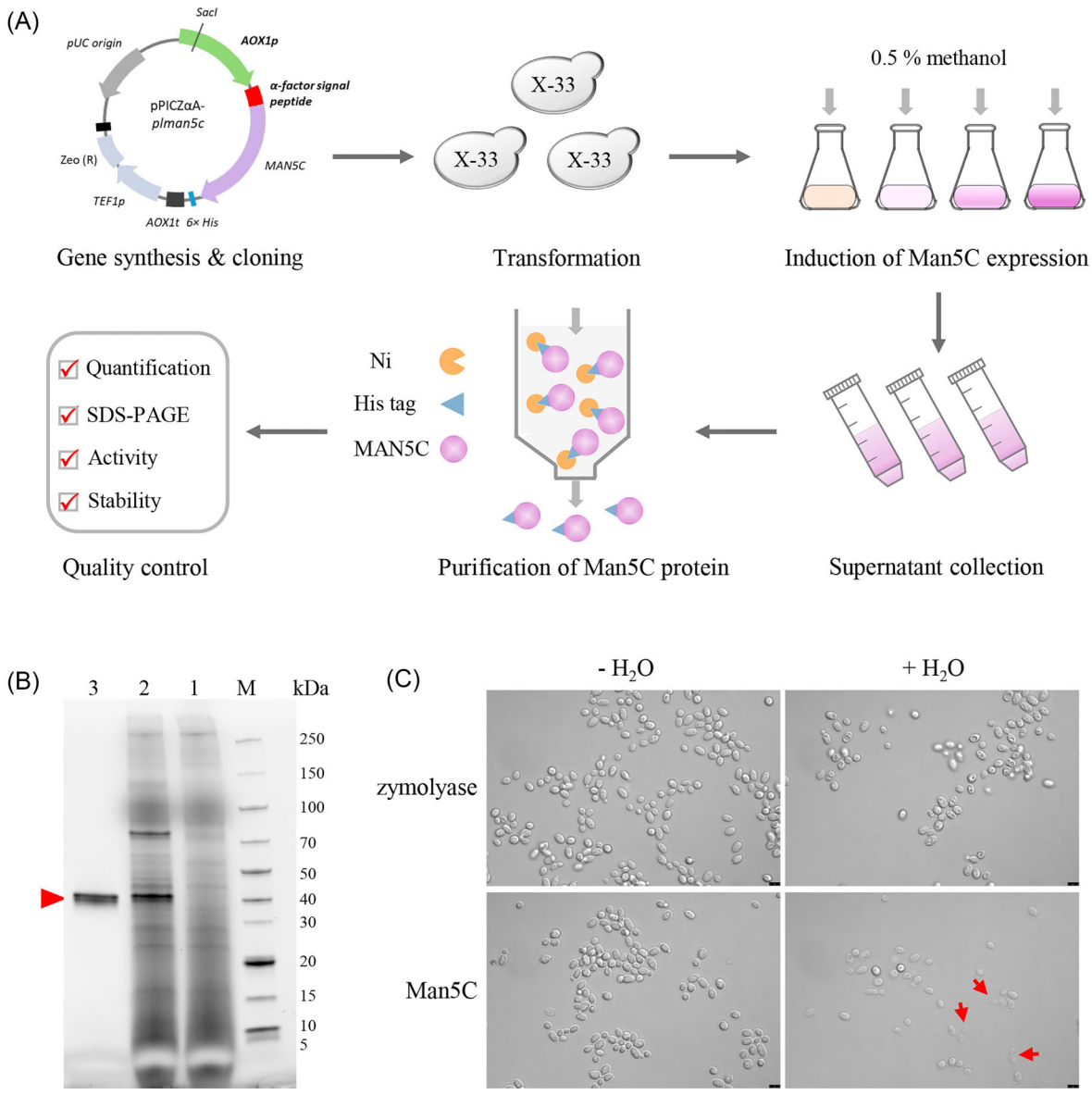

Figure 3 Production and application of recombinant Man5C protein for *R. toruloides* cell wall digestion. (A) Schematic workflow for the production and purification of Man5C in *P. pastoris* X-33. (B) SDS-PAGE analysis of Man5C expression. Lane M: protein marker; lane 1: concentrated supernatant from the control strain harboring an empty plasmid; lane 2: concentrated supernatant from the Man5C-expression strain; lane 3: purified Man5C protein. (C) Micrograph of *R. toruloides* BOT-A2 cells after 90 min of treatment with either zymolyase or Man5C at 37°C. Arrows indicate spherical cells with blurred boundaries following addition of H_2O. Scale = 5 μm.

codon-optimized *MAN5C* gene in *Pichia pastoris* (Fig. 3A). Using an N-terminal α-factor secretion signal and a C-terminal His tag, the recombinant protein was secreted into the culture medium and purified via affinity chromatography (Fig. 3B).

To assess the enzymatic activity of Man5C, protoplasts were prepared from the *R. toruloides* BOT-A2 strain. Cells were resuspended in an equal volume mixture of 10 mM sodium acetate (pH 4.5) and 0.9 M sodium citrate buffer (pH 7.5). Purified Man5C protein was added to a final concentration of 6.7 μg ml^{-1}, and the mixture was incubated at 30°C for 90 min. Upon addition of water, spherical cells with blurred boundaries were observed under a microscope, followed by cell lysis, which confirmed the formation of protoplasts. In contrast, control treatment with zymolyase produced no morphological changes with and without water addition, indicating its ineffectiveness against the *R. toruloides* cell wall (Fig. 3C). Following digestion, up to 90% of the protoplasts were able to regenerate on regeneration plates. These results demonstrate that recombinant Man5C protein is effective for degrading the *R. toruloides* cell wall and generating viable protoplasts.

Optimization of conditions for protoplast transformation

Protoplast-mediated transformation relies on enzymatic removal of the complex cell wall to generate protoplasts capable of taking up exogenous DNA. In *R. toruloides*, the absence of a functional episomal plasmid system necessitates the use of linear DNA

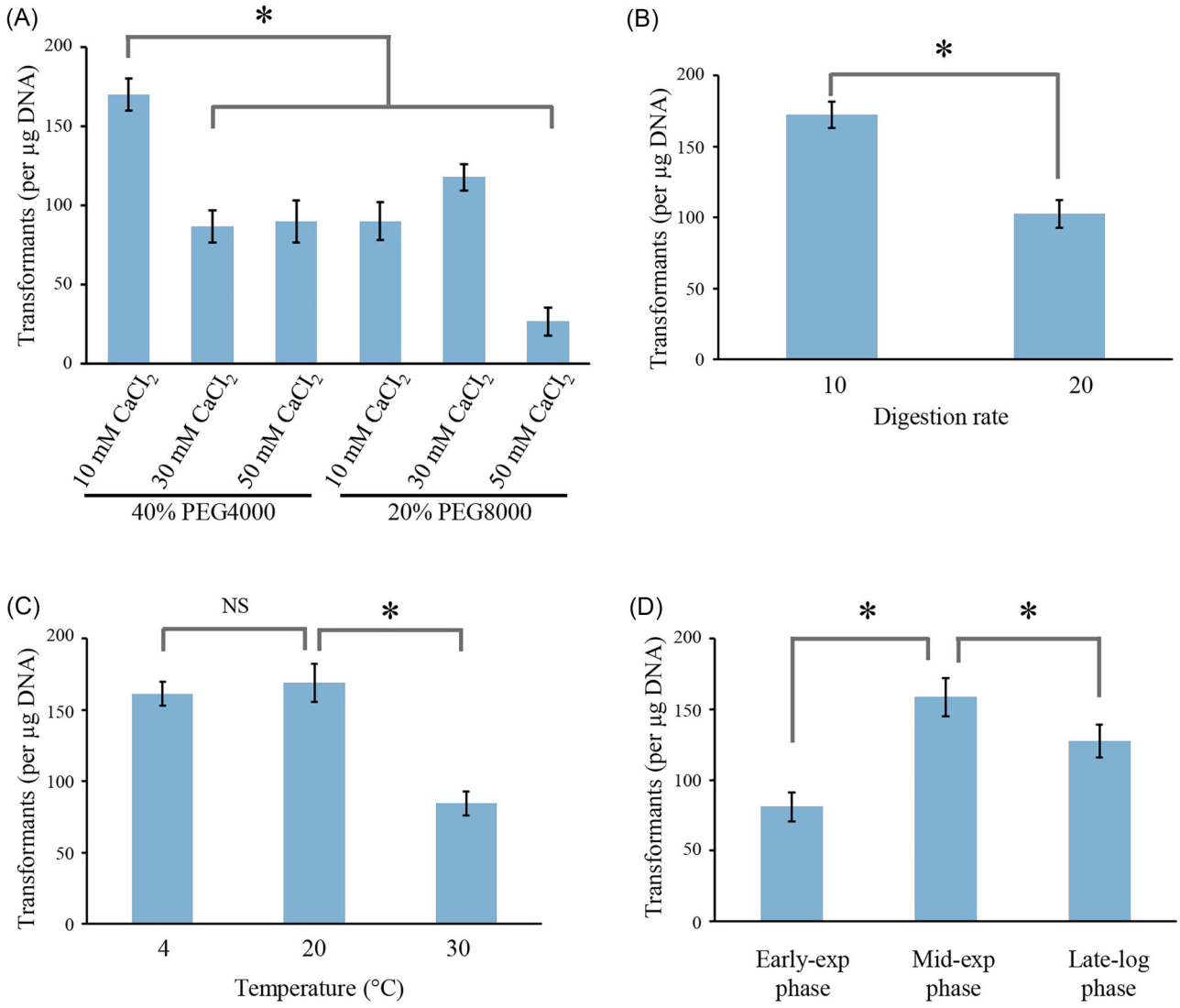

Figure 4 Optimization of protoplast transformation conditions for *R. toruloides* BOT-A2 strain. (A) Effects of PEG and calcium ion concentration. (B) Impact of cell wall digestion efficiency. (C) Effect of transformation temperature. (D) Influence of cell growth phase at the time of harvesting for transformation. Data are presented as the mean ± SD from three independent biological replicates. Asterisks (*) indicate statistically significant differences (P value < 0.05). NS indicates no significant difference (P value > 0.05).

fragments for transformation. In addition, non-homologous end-joining (NHEJ) is the major mechanism mediating chromosomal integration in *R. toruloides* (Schultz et al. 2019), resulting in random integration of linear DNA fragments into the genome. These features further increase the importance of optimizing transformation and selection parameters. The hygromycin B resistance gene, a widely used selection marker in fungal genetics, has been shown to be effective in *R. toruloides* (Xu et al. 2025, Zheng et al. 2025) and was used in this study as a linear Hyg resistance cassette. The optimal hygromycin B concentration for selection of BOT-A2 transformants was first determined to be 60 μg ml^{-1} (Supplementary Fig. 2), which is slightly higher than the 50 μg ml^{-1} previously reported for other strains (Xu et al. 2025, Zheng et al. 2025).

Although viable protoplasts were successfully generated using recombinant Man5C protein, no stable transformants were obtained until the digestion buffer was modified: replacing 0.9 M sodium citrate buffer (pH 7.5) with 1 M sorbitol. This substitution significantly improved protoplast generation, reducing the digestion time from 90 min to less than 30 min and decreasing the required Man5C concentration from 6.7 μg ml^{-1} to 1.12 μg ml^{-1}.

PEG and calcium ions play crucial roles in promoting DNA uptake during protoplast transformation. Both PEG molecular weight and calcium concentration require species- and sometimes strain-specific optimization. To evaluate their effects, 40% PEG 4000 and 20% PEG 8000 solution were each supplemented with 10 mM, 30 mM, or 50 mM $CaCl_2$, respectively. The highest transformation efficiency with 170 transformants per μg of DNA was achieved using 40% PEG 4000 with 10 mM $CaCl_2$. The second highest efficiency, 118 transformants per μg of DNA, was obtained with 20% PEG 8000 and 30 mM $CaCl_2$ (Fig. 4A and Supplementary Fig. 3). Based on these results, subsequent transformations were carried out using 40% PEG 4000 with 10 mM $CaCl_2$.

The extent of cell wall digestion is a critical factor, as over-digestion can significantly reduce transformation efficiency. To evaluate its impact, transformations were performed at two digestion endpoints, defined by OD_{600} ratio (pre- and post- Man5C

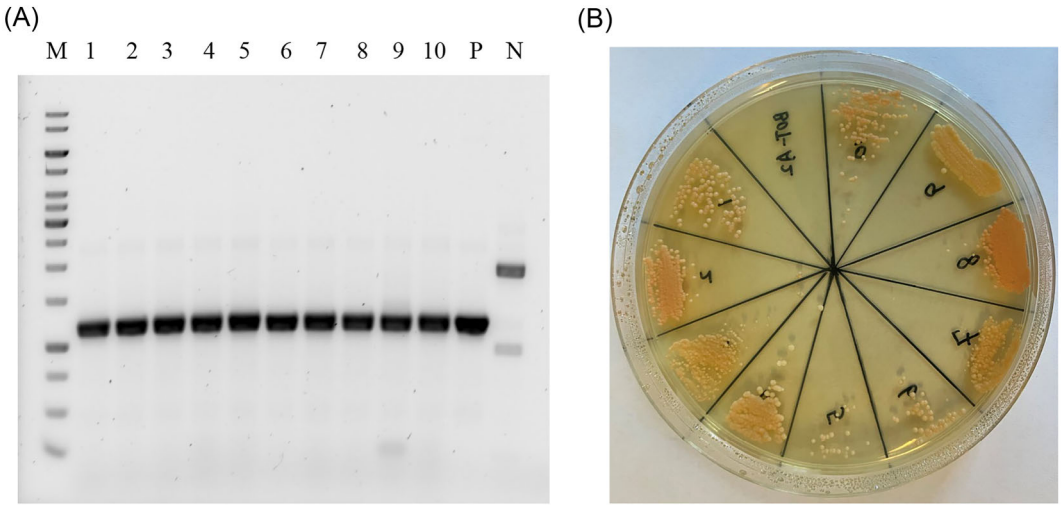

Figure 5 Verification of transformants after protoplast transformation. (A) PCR verification of transformants with chromosome integration of the hygromycin B resistance cassette. P indicates positive control using the NM1-5S-tRNA-SgH plasmid as template. N indicates negative control using BOT-A2 genomic DNA as template. (B) Genetic stability analysis of transformants after five consecutive serial passages.

digestion) of ~ 10 and 20, as described in Materials and Methods. A ratio of 10 yielded 172 transformants per μg of DNA, which was significantly higher than the 101 transformants per μg of DNA obtained at a ratio of 20 (Fig. 4B and Supplementary Fig. 4).

The incubation temperature during the PEG-mediated DNA uptake step is an important parameter affecting transformation efficiency and may vary depending on the strain and experimental conditions. To determine the optimal temperature, protoplasts were incubated with the transformation mixtures at 0°C, 20°C, and 30°C, respectively. Transformation efficiency was similar at 0°C and 20°C, both significantly higher than at 30°C (Fig. 4C).

Optimization of cell growth phase for cell collection

The growth phase at which *R. toruloides* cells were harvested for protoplast transformation had a substantial effect on transformation efficiency. Cells collected during the mid-exponential phase yielded the highest efficiency, with 159 transformants per μg of DNA. In comparison, cells from the early exponential and late-log phases produced 81 and 128 transformants per μg of DNA, respectively (Fig. 4D). This trend differs from previous studies in *R. toruloides* using lithium acetate transformation (Liu et al. 2023) and electroporation (Liu et al. 2017), where the highest efficiency was observed with early exponential phase cells.

We also observed that cell wall digestion time varied with growth phase: late-log phase cells required 42 min, compared to 26 min for mid-exponential and 18 min for early exponential phase cells. Based on findings in *S. cerevisiae* showing that osmotic stabilization of early exponential cells in 1 M ice-cold sorbitol overnight improves transformation efficiency (Zhang et al. 2019), we applied a similar treatment. Early and mid-exponential phase cells were incubated overnight at 4°C in 1 M sorbitol with gentle agitation. As a result, transformation efficiency for early exponential cells significantly increased from 81 to 190 transformants per μg of DNA, while no significant change was observed for mid-exponential phase cells.

To effectively eliminate false positives, transformants were cultivated in liquid medium under selective pressure, as the BOT-A2 strain exhibits higher resistance on solid selective medium (Supplementary Fig. 5A and 5B). Integration of the Hyg resistance cassette into the genome was then verified by PCR, with a fragment corresponding to the hygromycin B resistance gene detected in all ten randomly selected transformants (Fig. 5A). These transformants maintained resistance to hygromycin B after five consecutive serial passages in liquid YPD medium without selection pressure, indicating stable integration of the cassette (Fig. 5B and Supplementary Fig. 6).

General applicability of the protoplast transformation method

To evaluate the broader applicability of the linear DNA fragment-based protoplast transformation protocol, G418 and bleomycin resistance cassettes were tested (Fig. 6A). Optimal selection concentrations were first determined, following the same procedure used for hygromycin B. The effective concentrations were 80 μg ml^{-1} for G418 and 220 μg ml^{-1} bleomycin (Supplementary Fig. 7), which differ significantly from previously reported values of 200 μg ml^{-1} for G418 and 50 μg ml^{-1} for bleomycin (Liu et al. 2017, Schultz et al. 2019), indicating inherent strain-specific resistance profiles. Following transformation, 244 and 226 transformants per μg of DNA were obtained using G418 and bleomycin cassettes, respectively (Fig. 6B). These transformants maintained stable antibiotic resistance after five consecutive serial passages (Fig. 6C, D, and Supplementary Fig. 6).

To test strain compatibility, the protocol was also applied to the NP11 strain. However, no transformants were obtained under the same conditions. Compared to BOT-A2, NP11 exhibited slower growth in both YPD and YNB medium, with maximum growth rates of 0.374 vs. 0.444 in YPD (Fig. 7A and B) and 0.204 vs. 0.297 in YNB (Fig. 7C and D), respectively. Moreover, NP11 cells from mid-exponential phase required only 10 min for cell wall digestion, significantly shorter than the 26 min needed for BOT-A2 strain, sug-

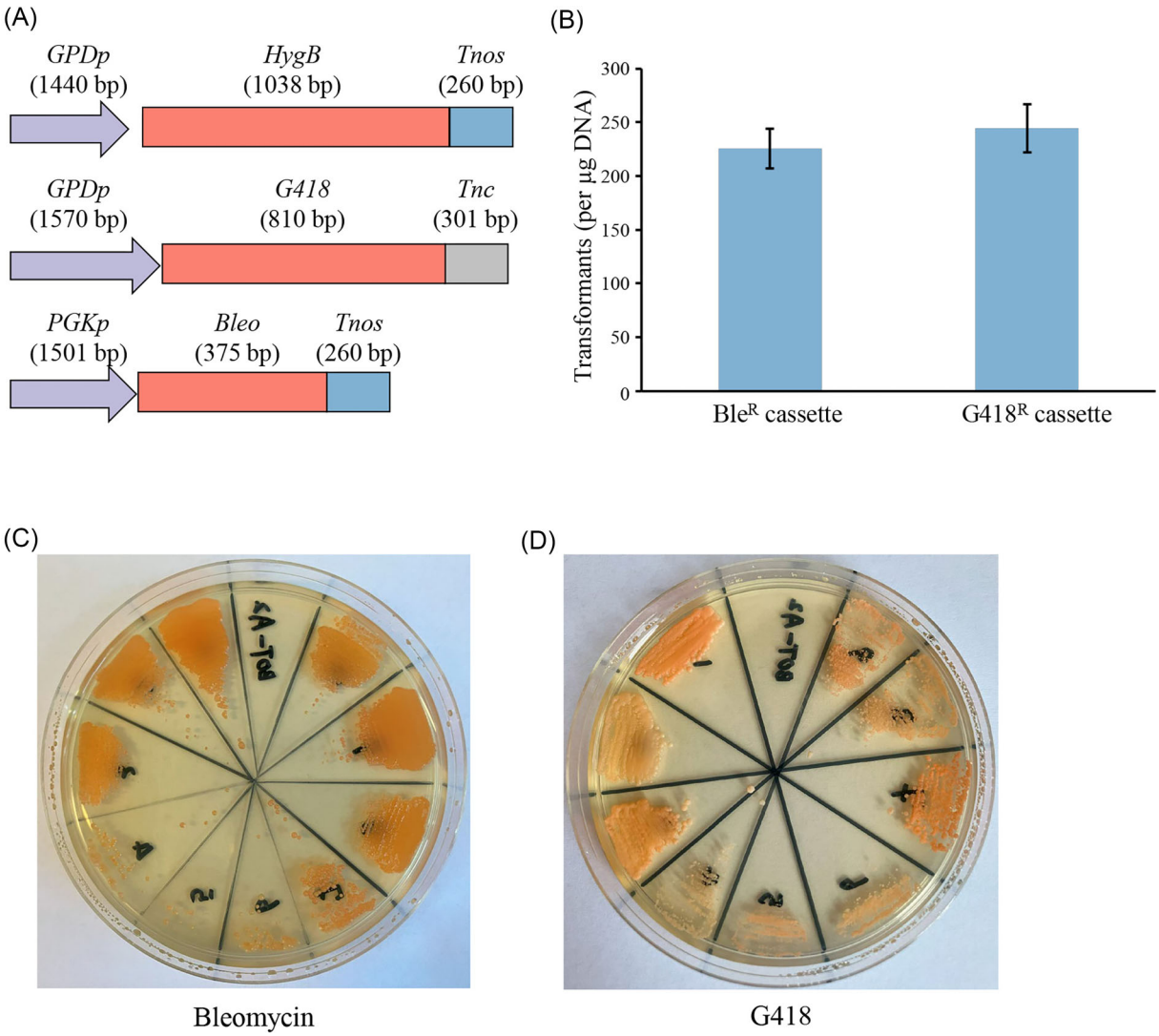

Figure 6 Protoplast transformation of *R. toruloides* BOT-A2 with G418 and bleomycin resistance cassettes. (A) Schematic illustration of the linear hygromycin B, G418, and bleomycin resistance cassettes used in this study. (B) Transformation efficiency of bleomycin B and G418 resistance cassettes. Data are presented as the mean ± SD from three independent biological replicates. (C, D) Genetic stability analysis of transformants harboring the bleomycin (C) and G418 (D) resistance cassettes after five consecutive serial passages.

gesting differences in cell wall composition. These physiological and growth differences, along with potential variation in antibiotic tolerance, highlight the need for strain-specific optimization to achieve efficient protoplast transformation.

Discussion

Fungal transformation is essential for both fundamental studies in molecular biology and the genetic manipulation of strains with industrial relevance. Among the available methods, PMT remains one of the most widely employed techniques, particularly when introducing large DNA fragments or when high transformation efficiency is required, such as transformation of a genomic plasmid library (Zhang et al. 2019). However, the success of PMT depends heavily on the efficient generation of protoplasts, which remains a challenge due to limited knowledge of lytic enzymes needed to digest fungal cell walls. This difficulty is further compounded in certain natural isolates or highly adapted industrial strains (often referred to as “domesticated strains”), which may have altered cell wall compositions (Machida et al. 2005, Jami et al. 2010). As a result, standard protoplast preparation protocols optimized for standard laboratory strains often fail to yield satisfactory results in these genetically divergent backgrounds.

In 1985, Tully *et al.* reported protoplast transformation of *R. toruloides* using a crude cell wall-degrading enzyme extract from *Paecilomyces lilacinus* ATCC36010 (Tully and Gilbert 1985). The lytic activity was later attributed to a β-1,3-glucomannanase encoded by the *MAN5C* gene, which specifically cleaves the β-1,3 glycosidic bonds in glucomannan, the main cell wall component of *R. toruloides* (Arai et al. 1978, Sugino et al. 2004). The recombinant Man5C protein was subsequently heterologously expressed in *P. pastoris* and its enzymatic activity was biochemically characterized (Yang et al. 2011). Building on this knowledge, *R. toruloides*

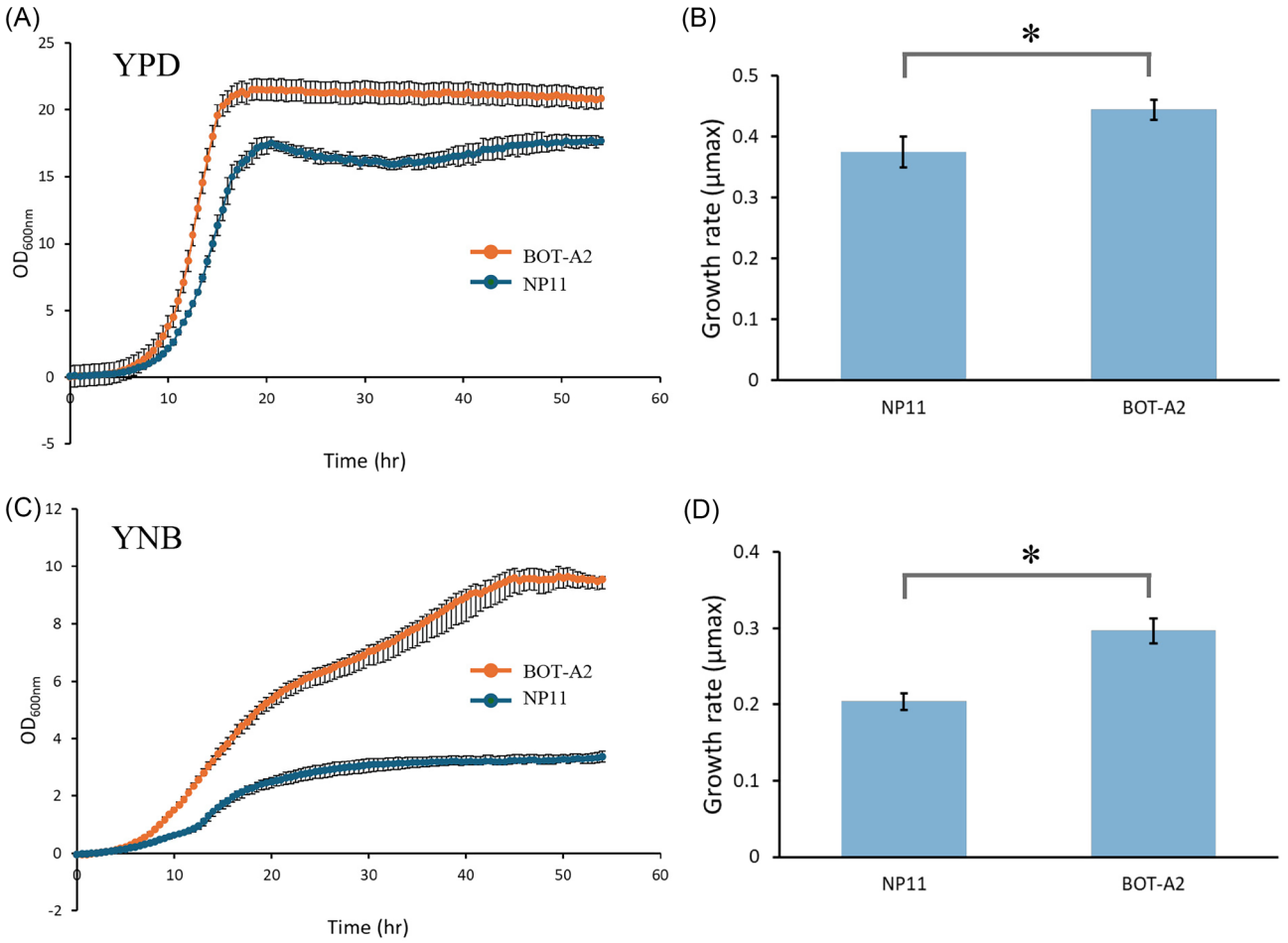

Figure 7 Comparison of cell growth between *R. toruloides* BOT-A2 and NP11 strains. (A) Growth curve of BOT-A2 and NP11 strains in YPD medium. (B) Maximum growth rates of BOT-A2 and NP11 strains in YPD medium. (C) Growth curve of BOT-A2 and NP11 strains in YNB medium. (D) Maximum growth rates of BOT-A2 and NP11 strains in YNB medium. For growth analysis, overnight cultures were diluted to an initial OD_{600} of 0.1 in fresh YPD or YNB medium, and cell growth was monitored at 30°C using a BioLector microcultivation system. Results shown are average values ± SD from three independent biological replicates. Asterisks (*) indicate statistical significance at P value < 0.05.

NP11 was later engineered for secretory expression of Man5C to promote partial cell wall degradation, achieving up to 93% lipid extraction efficiency (Liang et al. 2023). Following a similar protocol, we successfully expressed Man5C and generated viable protoplasts of the BOT-A2 strain (Fig. 3).

Although *R. toruloides* cells can regenerate after cell wall removal, successful selection of transformants also requires expression of the antibiotic resistance gene, making the process more complex than simple regeneration. In our study, protoplasts prepared using a 1:1 mixture of 10 mM sodium acetate (pH 4.5) and 0.9 M sodium citrate buffer (pH 7.5) failed to yield any transformants, suggesting that this buffer system may be suboptimal for supporting both protoplast viability and transformation efficiency. Sodium citrate at high concentrations may play dual roles during protoplast preparation. First, as a chelating agent, it may weaken the fungal cell wall by sequestering divalent cations such as Ca^{2+} and Mg^{2+}. Second, it may serve as an osmotic stabilizer, similar to sorbitol. However, PEG-mediated transformation is known to be sensitive to both ionic strength and the presence of chelators (Watanabe et al. 1992). Residual sodium citrate may sequester free Ca^{2+} ions, potentially interfering with DNA uptake during the transformation steps. In addition, the relatively high pH of the buffer mixture may lead to suboptimal conditions for enzymatic digestion, as the optimal activity of Man5C is around pH 4.5 (Yang et al. 2011). This may necessitate prolonged digestion time and higher enzyme concentrations. Indeed, replacing 0.9 M sodium citrate buffer (pH 7.5) with 1 M sorbitol significantly improved protoplast transformation efficiency, reducing the incubation time from 90 min to under 30 min, and lowering the required Man5C concentration from 6.7 μg ml^{-1} to 1.12 μg ml^{-1}.

DNA uptake during protoplast transformation is primarily mediated by PEG in the presence of calcium ions. PEG disrupts the plasma membrane integrity and facilitates the fusion of exogenous DNA with the protoplast membrane. Calcium ions are believed to stabilize DNA-membrane interactions and may promote internalization through PEG-induced endocytosis (Martín 2015). PEGs of different molecular weights, such as PEG 4000 and PEG 8000, are commonly used in fungal systems, with variations in viscosity and membrane fusion capacity. The optimal combination of

PEG molecular weight and calcium ion concentration varies across fungal species. In our study, the highest transformation efficiency was achieved using 40% PEG 4000 combined with 10 mM $CaCl_2$ (Fig. 4A and Supplementary Fig. 3). This condition aligns with protocols reported for *S. cerevisiae* and *K. lactis* (Hinnen et al. 1978, Sreekrishna et al. 1984), but differs from those optimized for *S. pombe* (20% PEG 4000 with 10 mM $CaCl_2$) and *P. pastoris*, where 20% PEG3350 with 10 mM $CaCl_2$ has been shown to be effective (Cregg et al. 1985, Moreno et al. 1991).

Successful regeneration following DNA uptake is a critical step in protoplast transformation, and the optimal conditions for this process can vary among fungal species. In *R. toruloides*, where a functional episomal plasmid system has not yet been established, we performed protoplast transformation using linear heterologous DNA fragments, which require chromosome integration to confer stable expression. Unlike plasmid-based systems, integration of linear DNA typically requires a longer recovery time before cells are capable of growing on selective medium. In our study, no stable transformants were obtained during recovery incubations of up to 6 h, and OD_{600} values remained unchanged. Notably, a marked increase in transformant numbers was observed after overnight recovery (∼14–16 h). This may suggest a potential enhancement in transformation efficiency, possibly due to more effective DNA integration and expression of the selective marker.

The BOT-A2 strain exhibited greater tolerance to hygromycin B on solid selective medium (Supplementary Fig. 5), suggesting that additional screening strategies may further improve the reliability and efficiency of transformant identification. In future studies, incorporation of fluorescent reporter systems, such as GFP or mCherry, alongside antibiotic selection markers could facilitate separation of true transformants from false-positive colonies during selection. Such reporter systems could provide a rapid and visually distinguishable method to assess exogenous gene integration and expression in *R. toruloides*.

In summary, we established an optimized protoplast transformation method for the *R. toruloides* BOT-A2 strain using linear DNA fragments (Supplementary materials). This method is expected to facilitate both metabolic engineering for industrial applications and fundamental research on this promising yeast in future studies.

Acknowledgements

We thank Prof. Thomas Andlid (Chalmers University of Technology, Sweden) for kindly providing the natural yeast isolate *R. toruloides* BOT-A2 stain. We are grateful to Professor Zongbao Kent Zhao (Dalian University of Technology, China) for providing the *R. toruloides* Y4 and NP11 strains and the pZPK-SaCas9 plasmid. We also thank Professor Huimin Zhao (University of Illinois at Urbana-Champaign, USA) for providing the NM1-5S-tRNA-SgH and NM9-SpCas9-NLS3 plasmids via Addgene. We thank Docent Yun Chen, Professor Shuobo Shi, Dr. Rui Pereira, Dr. Juan Liu, Dr. Xiang Jiao, Dr. Lingyun Li, Baisong Tong, Dr. Xiaozhi Fu, Dr. Lei Shi, Dr. Maximilian Otto, and Dr. Golnaz Mobasseri for their valuable discussions and comments. The graphical abstract was created using BioRender.com.

Author contribution

X.C. and V.S. conceived and designed the study. X.C. carried out experiments and wrote the paper. V.S. edited the paper.

Supplementary material

Supplementary material is available at *FEMSYR Journal* online.

Conflicts of interest

None declared.

Funding

This work was financially supported by the Novo Nordisk Foundation with grant numbers NNF20CC0035580 and NNF23OC0086516 as well as the Swedish Foundation for Strategic Research (grant number FFF20-0027).

Data availability

Data is available from the corresponding author upon reasonable request.

References

Antunes M, Mota MN, Fernandes PAR *et al.* Cell wall alterations occurring in an evolved multi-stress tolerant strain of the oleaginous yeast *Rhodotorula toruloides*. *Sci Rep* 2024;**14**:23366. https://doi.org/10.1038/s41598-024-74919-y.

Arai M, Lee TH, Murao S. Substrate specificity of the *Penicillium lilacinum* enzyme lytic to the cell wall of *Rhodotorula glutinis* and the structure of the *Rhodotorula* cell wall glucomannan. *Curr Microbiol* 1978;**1**:185–8. https://doi.org/10.1007/BF02601675.

Brink DP, Mierke F, Norbeck J *et al.* Expanding the genetic toolbox of *Rhodotorula toruloides* by identification and validation of six novel promoters induced or repressed under nitrogen starvation. *Microb Cell Fact* 2023;**22**:160. https://doi.org/10.1186/s12934-023-02175-2.

Cao M, Tran VG, Qin J *et al.* Metabolic engineering of oleaginous yeast *Rhodotorula toruloides* for overproduction of triacetic acid lactone. *Biotech & Bioengineering* 2022;**119**:2529–40. https://doi.org/10.1002/bit.28159.

Cregg JM, Barringer KJ, Hessler AY *et al. Pichia pastoris* as a host system for transformations. *Mol Cell Biol* 1985;**5**:3376–85.

Geiselman GM, Zhuang X, Kirby J *et al.* Production of ent-kaurene from lignocellulosic hydrolysate in *Rhodosporidium toruloides*. *Microb Cell Fact* 2020;**19**:24. https://doi.org/10.1186/s12934-020-1293-8.

Gietz RD, Woods RA. Genetic transformation of yeast. *BioTechniques* 2001;**30**:816–31, 822-816, 828 passim. https://doi.org/10.2144/01304rv02.

Hinnen A, Hicks JB, Fink GR. Transformation of yeast. *Proc Natl Acad Sci USA* 1978;**75**:1929–33. https://doi.org/10.1073/pnas.75.4.1929.

Hu C, Zhao X, Zhao J *et al.* Effects of biomass hydrolysis by-products on oleaginous yeast *Rhodosporidium toruloides*. *Bioresour Technol* 2009;**100**:4843–7. https://doi.org/10.1016/j.biortech.2009.04.041.

Hu J, Ji L. Draft genome sequences of *Rhodosporidium toruloides* strains ATCC 10788 and ATCC 10657 with compatible mating types. *Genome Announc* 2016;**4**:e00098–00016. https://doi.org/10.1128/genomeA.00098-16.

Jami MS, Barreiro C, García-Estrada C *et al.* Proteome analysis of the penicillin producer *Penicillium chrysogenum*: characterization of protein changes during the industrial strain improvement. *Mol Cell Proteomics* 2010;**9**:1182–98. https://doi.org/10.1074/mcp.M900327-MCP200.

Jiao X, Zhang Y, Liu X *et al.* Developing a CRISPR/Cas9 system for genome editing in the basidiomycetous yeast *Rhodosporidium toruloides*. *Biotechnol J* 2019;**14**:e1900036. https://doi.org/10.1002/biot.201900036.

Kirby J, Geiselman GM, Yaegashi J *et al.* Further engineering of *R. toruloides* for the production of terpenes from lignocellulosic biomass. *Biotechnol Biofuels* 2021;**14**:101. https://doi.org/10.1186/s13068-021-01950-w.

Koh CM, Liu Y, Moehninsi DM *et al.* Molecular characterization of KU70 and KU80 homologues and exploitation of a KU70-deficient mutant for improving gene deletion frequency in *Rhodosporidium toruloides*. *BMC Microbiol* 2014;**14**:50. https://doi.org/10.1186/1471-2180-14-50.

Kurtz MB, Cortelyou MW, Kirsch DR. Integrative transformation of *Candida albicans*, using a cloned Candida ADE2 gene. *Mol Cell Biol* 1986;**6**:142–9.

Li D, Tang Y, Lin J *et al.* Methods for genetic transformation of filamentous fungi. *Microb Cell Fact* 2017;**16**:168. https://doi.org/10.1186/s12934-017-0785-7.

Li Y, Zhao Z, Bai F. High-density cultivation of oleaginous yeast *Rhodosporidium toruloides* Y4 in fed-batch culture. *Enzyme Microb Technol* 2007;**41**:312–7. https://doi.org/10.1016/j.enzmictec.2007.02.008.

Liang S, Zhang Y, Lyu L *et al.* Secretory expression of β-1,3-glucomannanase in the oleaginous yeast *Rhodosporidium toruloides* for improved lipid extraction. *Bioresour Bioprocess* 2023;**10**:16. https://doi.org/10.1186/s40643-023-00639-2.

Liu D, Hwang HJ, Otoupal PB *et al.* Engineering *Rhodosporidium toruloides* for production of 3-hydroxypropionic acid from lignocellulosic hydrolysate. *Metab Eng* 2023;**78**:72–83. https://doi.org/10.1016/j.ymben.2023.05.001.

Liu H, Jiao X, Wang Y *et al.* Fast and efficient genetic transformation of oleaginous yeast *Rhodosporidium toruloides* by using electroporation. *FEMS Yeast Res* 2017;**17**:1–11. https://doi.org/10.1093/femsyr/fox017.

Lopes DD, Dien BS, Hector RE *et al.* Determining mating type and ploidy in *Rhodotorula toruloides* and its effect on growth on sugars from lignocellulosic biomass. *J Ind Microbiol Biotechnol* 2023;**50**:kuad040. https://doi.org/10.1093/jimb/kuad040.

Machida M, Asai K, Sano M *et al.* Genome sequencing and analysis of *Aspergillus oryzae*. *Nature* 2005;**438**:1157–61. https://doi.org/10.1038/nature04300.

Martín JF. 2015 Fungal transformation: from protoplasts to targeted recombination systems. *Genetic Transformation Systems in Fungi*, Vol. **1**, pp. 3–18. Cham: Springer International Publishing,

Moreno S, Klar A, Nurse P. Molecular genetic analysis of fission yeast *Schizosaccharomyces pombe*. *Methods Enzymol* 1991;**194**:795–823.

Qvirist L, Mierke F, Vazquez Juarez R *et al.* Screening of xylose utilizing and high lipid producing yeast strains as a potential candidate for industrial application. *BMC Microbiol* 2022;**22**:173. https://doi.org/10.1186/s12866-022-02586-y.

Sambles C, Middelhaufe S, Soanes D *et al.* Genome sequence of the oleaginous yeast *Rhodotorula toruloides* strain CGMCC 2.1609. *Genomics Data* 2017;**13**:1–2. https://doi.org/10.1016/j.gdata.2017.05.009.

Schultz JC, Cao M, Zhao H. Development of a CRISPR/Cas9 system for high efficiency multiplexed gene deletion in *Rhodosporidium toruloides*. *Biotech Bioeng* 2019;**116**:2103–9. https://doi.org/10.1002/bit.27001.

Schultz JC, Mishra S, Gaither E *et al.* Metabolic engineering of *Rhodotorula toruloides* IFO0880 improves C16 and C18 fatty alcohol production from synthetic media. *Microb Cell Fact* 2022;**21**:26. https://doi.org/10.1186/s12934-022-01750-3.

Sreekrishna K, Webster TD, Dickson RC. Transformation of *Kluyveromyces lactis* with the kanamycin (G418) resistance gene of Tn905. *Gene* 1984;**28**:73–81. https://doi.org/10.1016/0378-1119(84)90089-1.

Sugino H, Furuichi S, Murao S *et al.* Molecular characterization of a rhodotorula-lytic enzyme from paecilomyces lilacinus having beta-1,3-mannanase activity. *Biosci Biotechnol Biochem* 2004;**68**:757–60. https://doi.org/10.1271/bbb.68.757.

Todd RT, Braverman AL, Selmecki A. Flow cytometry analysis of fungal ploidy. *CP Microbiology* 2018;**50**:e58. https://doi.org/10.1002/cpmc.58.

Tsai Y-Y, Ohashi T, Kanazawa T *et al.* Development of a sufficient and effective procedure for transformation of an oleaginous yeast, *Rhodosporidium toruloides* DMKU3-TK16. *Curr Genet* 2017;**63**:359–71. https://doi.org/10.1007/s00294-016-0629-8.

Tully M&, Gilbert HJ. Transformation of *Rhodosporidium toruloides*. *Gene* 1985;**36**:235–40. https://doi.org/10.1016/0378-1119(85)90178-7.

Watanabe K, Kakita Y, Nakashima Y *et al.* Calcium requirement for protoplast transfection mediated by polyethylene glycol of Lactobacillus casei by PL-1 Phage DNA. *Biosci Biotechnol Biochem* 1992;**56**:1859–62. https://doi.org/10.1271/bbb.56.1859.

Xu H, Shi L, Boob AG *et al.* Discovery, characterization, and application of chromosomal integration sites for stable heterologous gene expression in *Rhodotorula toruloides*. *Metab Eng* 2025;**89**:22–32. https://doi.org/10.1016/j.ymben.2025.02.004.

Yang F, Zhang S, Jin G *et al.* Purification and characterization of a β-1,3-glucomannanase expressed in *Pichia pastoris*. *Enzyme Microb Technol* 2011;**49**:223–8. https://doi.org/10.1016/j.enzmictec.2011.04.005.

Zhang JJ, Yamanaka K, Tang X *et al.* Direct cloning and heterologous expression of natural product biosynthetic gene clusters by transformation-associated recombination. *Methods Enzymol* 2019;**621**:87–110.

Zhang Y, Kamal R, Li Q *et al.* Comparative Fatty Acid Compositional Profiles of *Rhodotorula toruloides* Haploid and Diploid Strains under Various Storage Conditions. *Fermentation* 2022;**8**:467. https://doi.org/10.3390/fermentation8090467.

Zheng X, Ledesma-Amaro R, Zhao ZK *et al.* Rhodotorula yeasts as potential chassis for sustainable food biotechnology. *J Agric Food Chem* 2025;**73**:19157–73. https://doi.org/10.1021/acs.jafc.5c05298.

Zhu Z, Zhang S, Liu H *et al.* A multi-omic map of the lipid-producing yeast *Rhodosporidium toruloides*. *Nat Commun* 2012;**3**:1112. https://doi.org/10.1038/ncomms2112.

Received: 26 March 2026. **Revised:** 30 May 2026. **Accepted:** 22 June 2026